Human Molecular Genetics, 2014, Vol. 23, No. 18 **4970–4984**
doi:10.1093/hmg/ddu212
Advance Access published on May 12, 2014

Comparison of epigenetic mediator expression and function in mouse and human embryonic blastomeres

Shawn L. Chavez[1,2,3,†], Sohyun L. McElroy[1,2,3], Nancy L. Bossert[4], Christopher J. De Jonge[4], Maria Vera Rodriguez[1,2,3,5], Denise E. Leong[1,2,3], Barry Behr[2], Lynn M. Westphal[2] and Renee A. Reijo Pera[1,2,3,*]

[1]Center for Reproductive and Stem Cell Biology, Institute for Stem Cell Biology and Regenerative Medicine, [2]Department of Obstetrics and Gynecology and [3]Department of Genetics, Stanford University School of Medicine, Stanford, CA 94305, USA, [4]Reproductive Medicine Center, University of Minnesota, Minneapolis, MN 55414, USA and [5]Iviomics, Valencia, Spain

Received January 31, 2014; Revised April 15, 2014; Accepted May 5, 2014

A map of human embryo development that combines imaging, molecular, genetic and epigenetic data for comparisons to other species and across pathologies would be greatly beneficial for basic science and clinical applications. Here, we compared mRNA and protein expression of key mediators of DNA methylation and histone modifications between mouse and human embryos, embryos from fertile/infertile couples, and following growth factor supplementation. We observed that individual mouse and human embryos are characterized by similarities and distinct differences in DNA methylation and histone modification patterns especially at the single-cell level. In particular, while mouse embryos first exhibited sub-compartmentalization of different histone modifications between blastomeres at the morula stage and cell sub-populations in blastocysts, differential histone modification expression was detected between blastomeres earlier in human embryos at the four- to eight-cell stage. Likewise, differences in epigenetic mediator expression were also observed between embryos from fertile and infertile couples, which were largely equalized in response to growth factor supplementation, suggesting that select growth factors might prevent alterations in epigenetic profiles during prolonged embryo culture. Finally, we determined that reduced expression via morpholino technologies of a single histone-modifying enzyme, Rps6ka4/Msk2, resulted in cleavage-stage arrest as assessed by time-lapse imaging and was associated with aneuploidy generation. Taken together, data document differences in epigenetic patterns between species with implications for fertility and suggest functional roles for individual epigenetic factors during pre-implantation development.

INTRODUCTION

Recent studies in mouse and human have explored molecular, genetic, epigenetic and imaging profiles of pre-implantation embryos at different stages during development (1–6). A fundamental component of mammalian pre-implantation development is the erasure and re-establishment of epigenetic marks (epigenetic reprogramming) (7). Following fertilization, the paternal and maternal genomes are extensively modified and reset prior to implantation, which is thought to be required to establish the totipotency of the newly formed embryo (8). The two main types of epigenetic mechanisms are DNA methylation and histone

*To whom correspondence should be addressed at: Stanford University, Institute for Stem Cell Biology and Regenerative Medicine, 265 Campus Drive West; Room 3021A, Stanford, CA 94305-5463, USA. Tel: +1 6507253803; Fax: +1 6507233825; Email: reneer@stanford.edu
†Present address: Division of Reproductive & Developmental Sciences; Oregon National Primate Research Center and Oregon Health & Science University, Beaverton, OR 97006, USA.

modifications, which work together to affect gene expression in a potentially heritable manner (without altering DNA sequence) and influence chromatin structure (9–11). DNA methylation is mediated by a family of DNA methyltransferases (DNMTs) that catalyze the transfer of a methyl group to the 5′-position of cytosine residues within CpG dinucleotides usually resulting in effective gene silencing (12). Although global DNA methylation patterns in pre-implantation development have been documented in several species, the elucidation of DNMT expression particularly in early human embryos is far from complete, with focus on just a few stages of pre-implantation development and/or particular DNMT family members (13–16). Histone modifications include, but are not limited to, the phosphorylation of serine residues, acetylation of lysine residues and the methylation of either lysine or arginine residues, all of which are mediated by different histone-modifying enzymes and may affect biological outcome (17). While some studies have analyzed a subset of histone modifications in pre-implantation embryos from different species, data remains limited, especially in the human (18–21).

In this study, we compared expression of key regulators of DNA methylation and histone modifications between the different stages of mouse and human pre-implantation development, between embryos from fertile and infertile couples, and following media supplementation with a growth factor cocktail. We then assessed function via reduction in expression of a particular epigenetic regulator implicated in both mouse and human pre-implantation development. Human embryos were obtained from a unique set that were cryopreserved at the one-cell stage prior to assessment of quality and thus, likely to be representative of 'fresh' embryos from conception cycles (22,23), which have been shown to have similar potential for successful development, implantation, pregnancy and delivery as previously described (24).

RESULTS

Differential DNMT and histone-modifying enzyme mRNA expression patterns in mouse and human embryos

We first examined which DNMTs were associated with different stages of pre-implantation development in mouse and human embryos (Fig. 1A and B). For this purpose, we evaluated *DNMT1*, *DNMT2*, *DNMT3A*, *DNMT3A2*, *DNMT3B* and *DNMT3L* expression in individual mouse or human embryos at the one-cell, two-cell, four-cell, eight-cell, morula and blastocyst stages by microfluidic quantitative RT-PCR (Q-PCR; Supplementary Material, Table S1). As shown in Figure 2A and Supplementary Material, Figure S1a, some differences in DNMT expression between mouse embryos were detected beginning at the two-cell stage when zygotic genome activation (ZGA) begins (25), until the eight-cell stage of development; less variation in DNMT expression patterns was observed between individual mouse one-cell, morula and blastocysts. In human embryos, greater variation in DNMT expression was detected between individual human embryos at the cleavage stage than in the mouse and this variation occurred later in development [between the four- and eight-cell stages, coincident with the major wave of embryonic genome activation (EGA; 3,26), and the morula stage; Fig. 2B and Supplementary Material, Fig. S1b]. Thus, no common DNMT expression pattern could be detected between mouse and human embryos, confirming the differences in global DNA methylation levels observed in each species (15,27–30).

We next examined the expression of enzymes that mediate particular histone modifications in both mouse and human pre-implantation embryos (Fig. 1A and B). To accomplish this, we focused on histone-modifying enzymes that are involved in the phosphorylation of serine residues [Aurora B Kinase (*AURKB*), Ribosomal Protein S6 kinase, 90 kDa, polypeptide

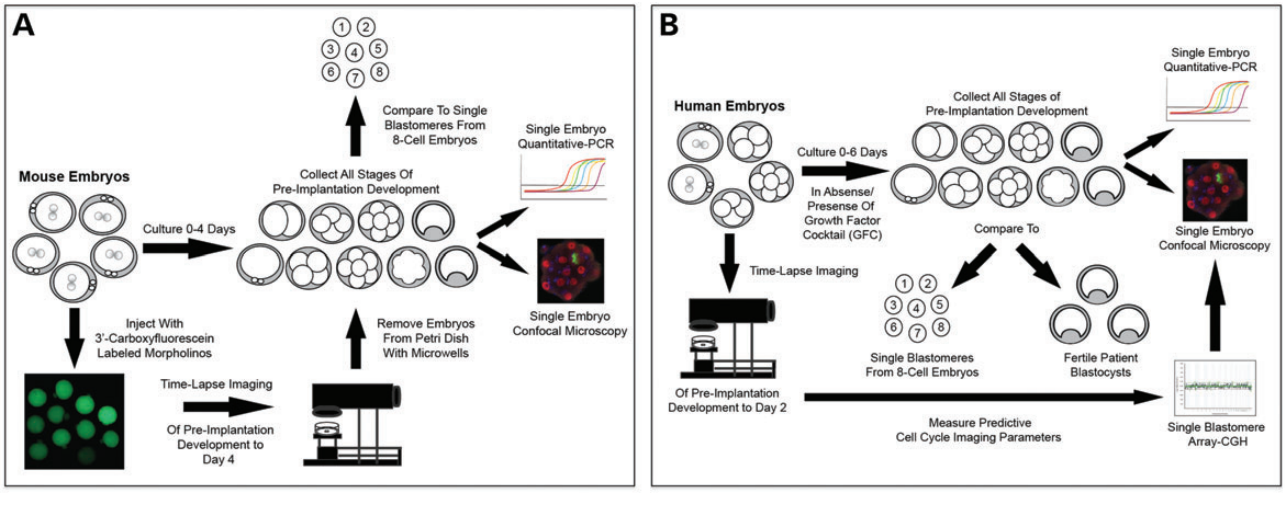

Figure 1. Experimental design of mouse and human embryo experiments in this study. (**A**) Non-injected mouse zygotes were cultured up to 4 days and all stages of pre-implantation development were collected for single-embryo Q-PCR or confocal microscopy. Similar Q-PCR analysis was also performed on single blastomeres from eight-cell mouse embryos on Day 3. Functional analysis of a particular epigenetic regulator was accomplished by microinjecting with 3′-carboxyfluorescein-labeled morpholinos and embryo development monitored by time-lapse imaging for comparison to non-injected embryos by Q-PCR and confocal microscopy. (**B**) Similar human embryo experiments were performed in the absence or presence of a growth factor cocktail (GFC) up to 6 days of culture with additional Q-PCR comparison to fertile patient blastocysts and functional assessment of human embryonic development via previously identified cell cycle parameters predictive of blastocyst formation and aneuploidy generation. The chromosomal status of single human blastomeres was evaluated by array-comparative genomic hybridization (A-CGH) for correlation to single blastomere gene expression results from the same embryo or by whole embryo confocal microscopy of micronuclei formation.

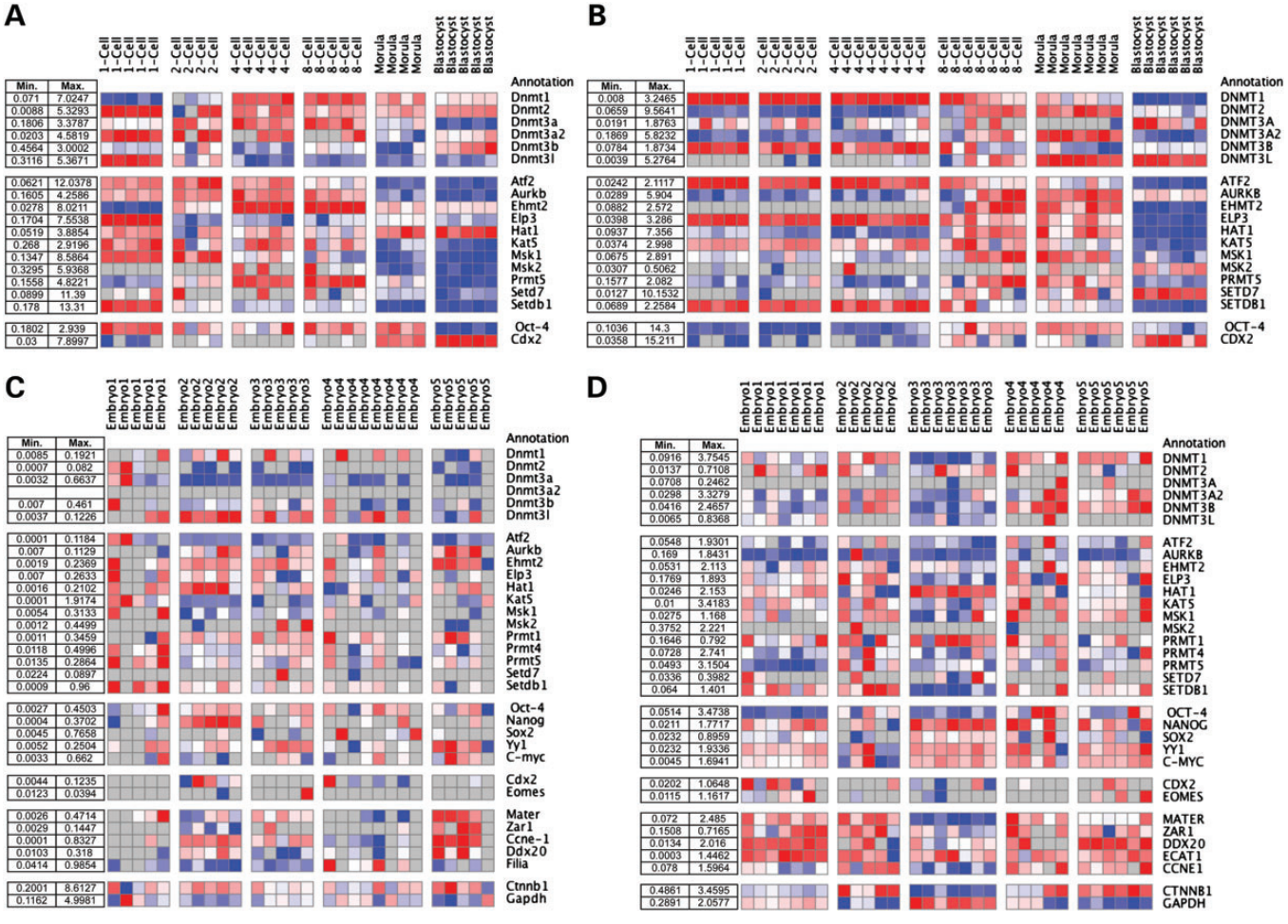

Figure 2. Epigenetic regulator expression in single mouse and human embryos and blastomeres. The expression of DNA methyltransferases (DNMTs), histone-modifying enzymes, *OCT-4* and *CDX2* was analyzed in (**A**) mouse and (**B**) human embryos throughout pre-implantation development by microfluidic Q-PCR. Cycle threshold (Ct) values were normalized to the most stable housekeeping genes and graphed for comparison between the two species. Similar Q-PCR analysis of DNMTs, histone-modifying enzymes and maternal effect, zygotic activation, pluripotency and housekeeping genes as well as cell lineage markers in individual blastomeres from Day 3 (**C**) mouse and (**D**) human embryos performed at approximately the eight-cell stage. Grey squares indicate no expression, whereas blue, white and red squares correspond to low, medium and high expression, respectively. The range of expression levels for each gene is as shown on the left with the minimum (Min.) and maximum (Max.) values. The graphs of non-normalized values are shown in Supplementary Material, Figure S1.

5 (*RPS6KA5*/*MSK1*) and *RPS6KA4*/*MSK2*], acetylation of lysine residues [activating transcription factor 2 (*ATF2*), K (lysine) acetyltransferase 5 (*KAT5*), Elongator complex protein 3 (*ELP3*)/*KAT9* and Histone acetyltransferase 1 (*HAT1*)/*KAT1*] and the methylation of either lysine residues [euchromatic histone-lysine *N*-methyltransferase 2 (*EHMT2*)/*G9A*, SET domain containing 7 (*SETD7*)/*KMT7* and SET domain bifurcated 1 (*SETDB1*)/*KMT1E*] or arginine residues [Protein arginine methyltransferase 5 (*PRMT5*)] (Supplementary Material, Table S1). Analogous to DNMT expression patterns, the levels and timing of expression of most histone-modifying enzymes differed between mouse and human embryos (Fig. 2A and B and Supplementary Material, Fig. S1a and b). Indeed, only *ATF2*, *KAT5*, *RPS6KA4*/*MSK2*, *PRMT5* and *SETDB1* were similarly expressed in mouse and human pre-implantation embryos. Moreover, the greatest differences in histone-modifying enzyme expression were detected in human embryos between the four- to eight-cell and morula stages. This variability in both DNMT and histone-modifying enzyme expression correlated with differences in the expression of the cell lineage regulators, POU class 5 homeobox 1 (*POU5F1*)/*OCT-4* and caudal-type homeobox 2 (*CDX2*), markers that have been shown to be predictive of inner cell mass (ICM) and trophectoderm lineage patterning (4,31), respectively (Fig. 2A and B and Supplementary Material, Fig. S1a and b).

Single-cell analysis of epigenetic regulators in cleavage-stage mouse and human embryos

We next sought to evaluate expression of epigenetic regulators in individual blastomeres from the same embryo. For this purpose, Day 3 mouse and human embryos were disassembled to single cells at approximately the eight-cell stage, a time when the embryonic genomes of both species should be activated (3,25,26), and DNMT and histone-modifying enzyme expression was analyzed by Q-PCR (Fig. 1A and B). While some transcripts such as *Dnmt3a2* were undetectable in individual blastomeres from mouse embryos, which may be due to less total RNA

in mouse versus human embryos (6,32), both mouse and human blastomeres exhibited a relatively similar degree of variation in DNMT and histone-modifying expression within the same embryo. This variation was also reflected in blastomere differences between *OCT-4* and *CDX2* expression as well as other pluripotency regulators, including NANOG Homeobox (*NANOG*), sex determining region Y-box 2 (*SOX2*), YIN-YANG-1 (*YY1*) and myelocytomatosis oncogene (*MYC*)/c-MYC, and trophectoderm regulators such as eomesodermin (*EOMES*) (Fig. 2C and D and Supplementary Material, Fig. S1c and d). However, differences in the expression of pluripotency, trophectoderm and epigenetic regulators were not universal to all genes expressed at this stage of development since little or no variation was observed in the expression of the maternal-effect genes, NLR family, pyrin domain containing 5 (*NLRP5*)/*MATER* and zygote arrest 1 (*ZAR1*), or the zygotic/EGA genes, DEAD box polypeptide 20 (*DDX20*)/*GEMIN3*, KH domain containing 3, subcortical maternal complex member (*Khdc3*)/*Filia* and KH domain containing 3-like, subcortical maternal complex member (*KHDC3L*)/*ECAT1* (Fig. 2C and D and Supplementary Material, Fig. S1c and d).

Analysis of histone modification sub-compartmentalization in mouse and human embryos

Using immunofluorescence and multi-color confocal microscopy analysis, we assessed changes in the expression of certain histone modifications in mouse and human embryos at the protein level (Fig. 1A and B). We focused our attention on the expression and localization of Histone H3 serine 10 phosphorylation (H3-S10P), H3-S28P, histone H4 lysine 16 acetylation (H4-K16acetyl) and histone H4 arginine 3 dimethylation (H4-R3me2) given that the mRNAs for the corresponding histone-modifying enzymes were expressed in mouse and human embryos. The expression of histone H3 lysine 4 trimethylation (H3-K4me3) was also evaluated since H4-R3me2 can be both a transcriptionally active and repressive mark (33,34). We validated specificity of the antibodies by immunofluorescence in the undifferentiated human embryonic stem cell (hESC) lines, H9 (XX) and HSF1 (XY) (Fig. 3A). Negative controls included single-color antibody staining to discount potential interference between different confocal channels as well as isotype controls (Supplementary Material, Fig. S2a and b).

Analysis of expression and localization of histone modifications in mouse embryos indicated that each blastomere exhibited similar epigenetic marks during the early cleavage stages of development both by single-frame confocal imaging (Fig. 3B and Supplementary Material, Fig. S3a) and three-dimensional modeling of Z-stacked confocal images (Fig. 3D). However, there were differences in the expression levels of the same histone modification between blastomeres within the same embryo (indicated by white-dashed arrow), which is in accordance with previous findings (19). As Figure 3B and Supplementary Material, Figure S3a demonstrate, it was not until later in development (between the morula and blastocyst stages) that sub-compartmentalization of different epigenetic marks such as H3-S28P and H4-R3me2 was observed between blastomeres or cell populations within the same embryo (shown by white solid arrows). Notably, we also observed H4-R3me2 and H3-K4me3 expression in one or both of the pronuclei and H3-S28P expression in one of the polar bodies in mouse embryos at the one-cell stage (Fig. 3B and Supplementary Material, Fig. S3a and c), suggesting that H3-S28P may be a marker of the first polar body since H3-S28P is associated with mitosis and the first polar body can undergo cytokinesis at least in the mouse (35). Expression of H3-S10P appeared to localize to small structures in the cytoplasm of cleavage-stage mouse embryos (Fig. 3B and D), which may be explained by previous findings that histones can bind strongly to isolated mitochondria, the phosphorylation of histone H3 is associated with mitosis and mitotic progression is closely integrated with mitochondrial dynamics (36–38). We also note differences in the expression pattern of H3-S10P as well as H4-K16acetyl to that of previous reports (39,40) and this is likely due to differences in fixation. The previous studies used methods that included fixation with paraformaldehyde, which is known to cause DNA–protein crosslinking and the loss of organelles such as mitochondria when combined with Triton X-100 for permeabilization (41,42), while methanol fixation was used in the present study to avoid histone crosslinking.

In contrast to mouse embryos, human embryos first exhibited differential histone modification expression patterns between blastomeres by the four- to eight-cell stages when analyzed by single-frame confocal imaging (Fig. 3B and Supplementary Material, Fig. S3b) or three-dimensional modeling of Z-stacked confocal images (Fig. 3D). Individual human blastomeres expressed either completely different histone modification marks such as H3-S28P and H4-R3me2 or were entirely devoid of histone modification expression observed in other blastomeres within the same embryo (indicated by white solid arrows). Similar to the mouse, however, sub-compartmentalization of histone modifications was also detected in human embryos later in development between blastomeres at the morula stage and within the ICM and trophectoderm sub-populations at the blastocyst stage (Fig. 3B and Supplementary Material, Fig. S3b). Immunostaining human embryos for H3-K4me3 also revealed a differential histone modification expression pattern at the eight-cell stage of human development in addition to positive signals for H3-K4me3 and H3-S28P in one of the pronuclei and polar bodies at the one-cell stage, respectively (Fig. 3C and Supplementary Material, Fig. S3b).

Reduced Rps6ka4/Msk2 expression induces mitotic arrest and micronuclei formation in mouse embryos

In order to determine whether specific histone-modifying enzymes were implicated in the progression of pre-implantation development beyond ZGA, we microinjected morpholino oligonucleotides (MOs) at the one-cell stage and monitored embryo development by time-lapse imaging (Fig. 1A). To facilitate an understanding of both mouse and human development, we initially focused our attention on the histone-modifying enzymes that were similarly expressed in both mouse and human embryos. However, *ATF2*, *KAT5*, *PRMT5* and *SETDB1* had multiple transcript variants, a high percentage of GC base content around the first exon and/or an atypical start codon, making MO design difficult for these histone-modifying enzymes (43). Given that relatively little is known about the role of serine phosphorylation in mammalian pre-implantation development and the importance of mitosis at the cleavage stage, we focused our efforts on *RPS6KA4*/*MSK2*, a mitogenic

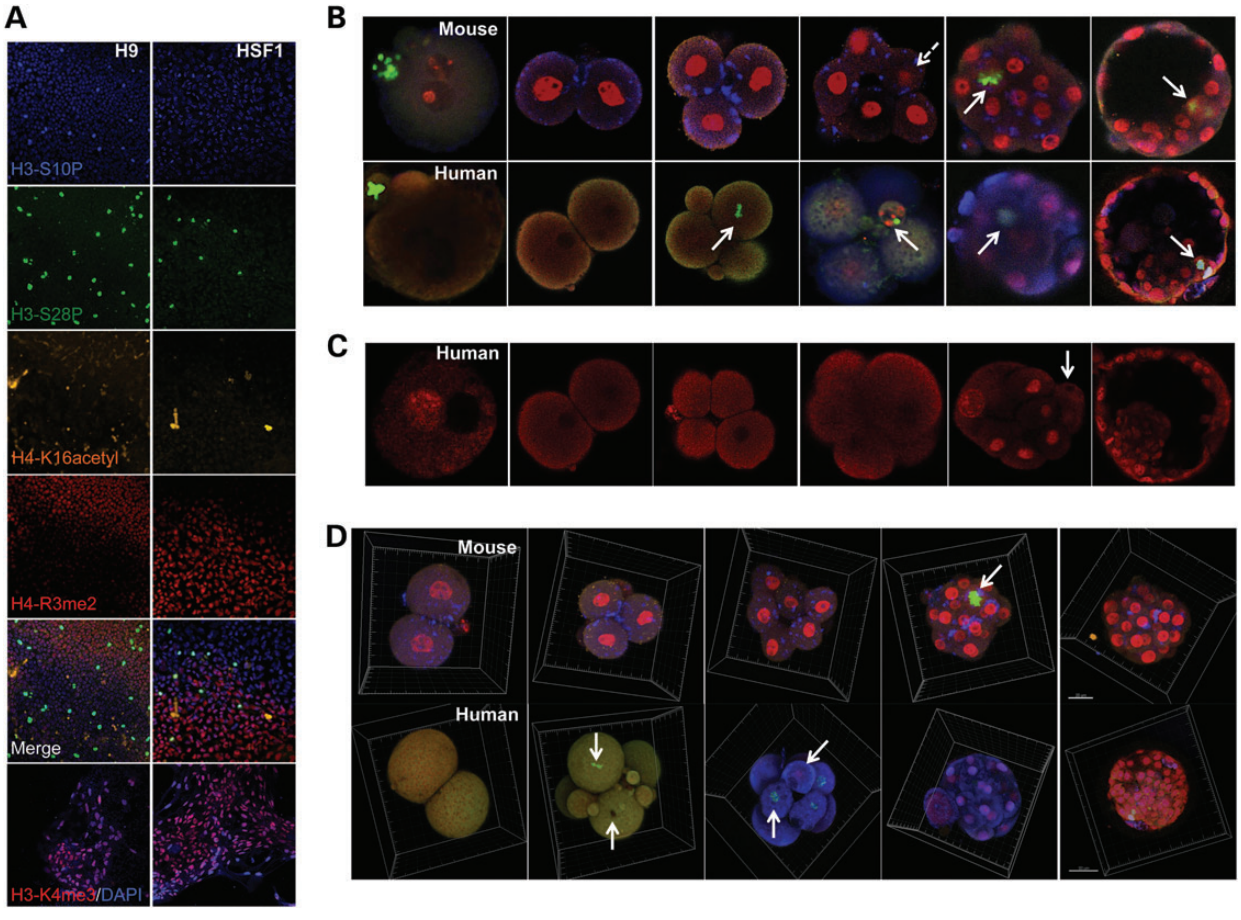

Figure 3. Multi-channel confocal analysis of histone modifications in mouse and human embryos. (**A**) Undifferentiated hESC lines (H9; XX and HSF1; XY) were immunostained with several different histone modification antibodies and Histone H3-S10P (blue), H3-S28P (green), H4-K16acetyl (orange) and H4-R3me2 (red) were chosen for further analysis based on their expression pattern. Since histone H4-R3me2 has been shown to be associated with both transcriptional activation and repression, the undifferentiated hESCs were also incubated with a primary antibody for Histone H3-K4me3 (red), a transcriptionally active mark, and DAPI (blue). Both H3-S10P and DAPI required the use of the blue confocal channel and, therefore, could not be analyzed simultaneously. (**B**) The expression and localization of histone H3-S10P, H3-S28P, H4-K16acetyl and H4-R3me2 was then analyzed in mouse and human embryos throughout pre-implantation development by multi-channel confocal microscopy ($n = 6–8$ embryos per stage). Note the difference in developmental stage when different histone modification sub-compartmentalization begins between mouse and human blastomeres in the same embryo (indicated by white solid arrows), although some differences in the expression level of the same histone mark such as H4-R3me2 is still observed in mouse embryos (shown by white-dashed arrows). (**C**) Similar confocal analysis of histone H3-K4me3 in human embryos exhibiting positive expression in one of the pronuclei at the zygote stage as well as certain blastomeres beginning at the eight-cell stage. (**D**) 3-D modeling of histone modifications in mouse and human embryos from the two-cell to blastocyst stage by Z-stack confocal microscopy demonstrating further evidence of differences in the timing of first sub-compartmentalization between the two species. Note that individual human blastomeres simultaneously expressed either completely different histone modification marks such as H3-S28P and H4-R3me2 or were entirely devoid of histone modification expression observed in other blastomeres within the same embryo at the four- to eight-cell stage (indicated by white solid arrows). The immunostaining controls and single-channel confocal analysis are shown in Supplementary Material, Figures S2 and S3, respectively; scale bar for mouse = 20 μm and for human = 50 μm.

factor that is known to be involved in the G1 phase of the cell cycle (44). We first sought to determine whether we could specifically knockdown Msk2 expression using a MO designed to target the translation start site of Msk2. To accomplish this, E8.5 mouse embryonic germ (mEG) cells, which express high levels of Msk2, were mock transfected or transfected with either a 3′-carboxyfluorescein-labeled standard control or 3′-carboxyfluorescein-labeled Msk2 morpholino (Msk2 MO) since analysis of Msk2 knockdown in pre-implantation embryos at the protein level would require several hundred embryos. Msk2 expression was analyzed by western blot 48–144 h later and showed that in contrast to the mock transfection or control MO, the nucleofected Msk2 MO knocked down Msk2 protein expression in 8.5mEGs (Fig. 4A).

Our next objective was to determine whether microinjection of the Msk2 MO using the injection of the 3′-carboxyfluorescein-labeled MO as a control had any effects on pre-implantation development. Initially, we determined that both non-injected and nuclease-free water-injected one-cell mouse embryos exhibited similar rates of blastocyst formation at ∼80%, while 75% blastocyst formation rates were observed in standard control injected embryos (Fig. 4B and C and Table 1) as demonstrated by time-lapse imaging (Supplementary Material, Movies S1 and S2). More importantly, when the gene expression profiles of non-injected and standard control injected blastocysts were compared, differences in the expression of only 2 out of the 50 genes tested could be detected (Supplementary Material, Fig. S4a). The two genes that were expressed at higher levels

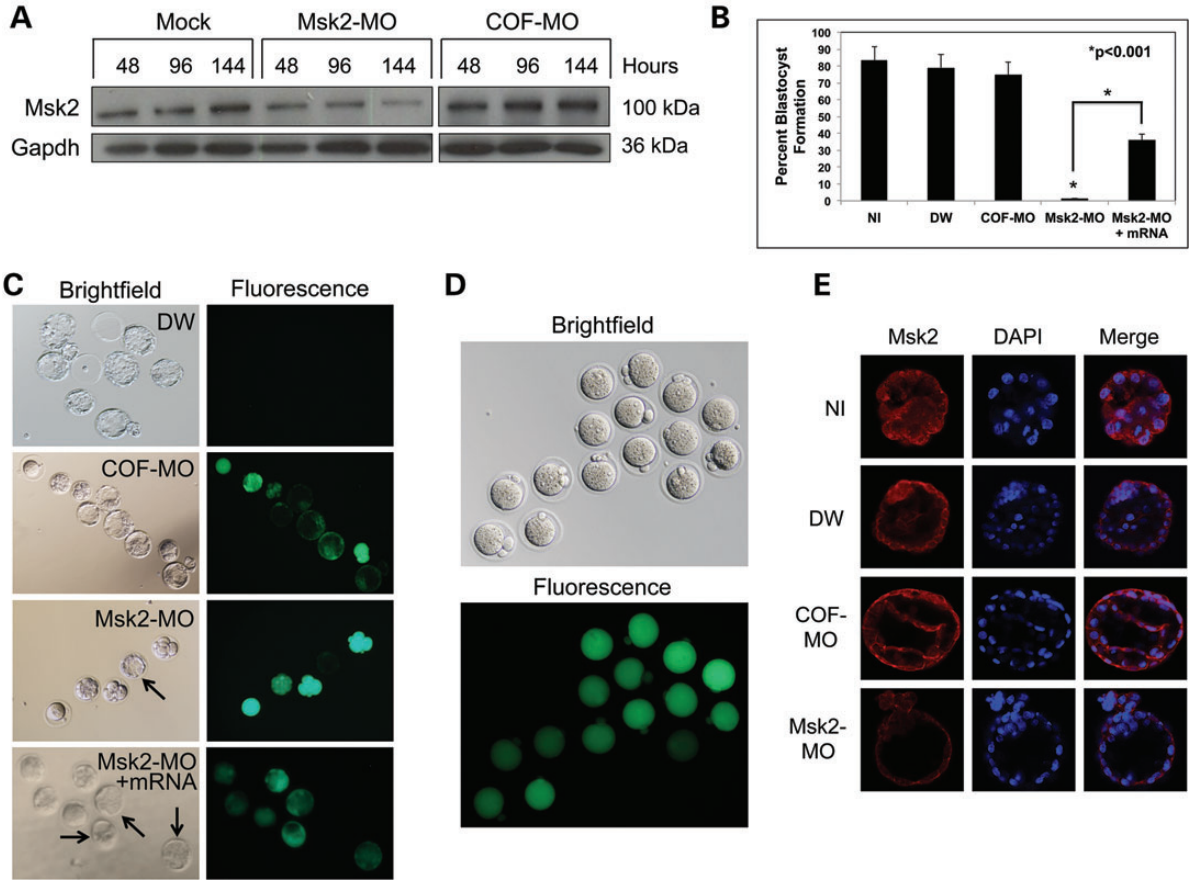

Figure 4. Knockdown of Msk2 expression reduces blastocyst formation rates. (**A**) The efficiency of Msk2 knockdown was first assessed by nucleofecting undifferentiated E8.5 mEG cells with water (mock), Msk2 morpholino (Msk2 MO) or 3′-carboxyfluorescein-labeled standard control morpholino (COF-MO) and Msk2 expression (100 kDa) evaluated using Gapdh (36 kDa) as a loading control by western blot analysis 48–144 h later. (**B**) Blastocyst formation rates were calculated for non-injected (NI; $n = 73$) as well as water (DW; $n = 19$), COF-MO ($n = 71$) and Msk2 MO ($n = 73$) injected mouse embryos. Graphic representation of the percentages for each experimental group, including the percent blastocyst formation following the co-injection of Msk2 MO and *Msk2* mRNA (Msk2 MO + mRNA; $n = 33$) in embryos is as shown and corresponds to Table 1. (**C**) Brightfield imaging and fluorescent microscopy of embryos in each group from one representative experiment. Note the single blastocyst observed following injection with the Msk2 MO (indicated by black arrow), (**D**) which may be explained by the amount of morpholino injected as revealed by slight differences in fluorescent intensities at the zygote stage. (**E**) Reduced Msk2 expression was detected in the single Msk2 MO-injected blastocyst obtained in comparison with the other experimental groups.

in non-injected embryos were the trophectoderm genes, *Cdx2* and *Eomes*, which may be explained by the finding that a delay (approximately 12 hours) in blastocyst formation was observed in control injected over non-injected embryos (Supplementary Fig. S4b and c).

We then evaluated the affects of Msk2-specific knockdown by comparing similar concentrations of Msk2 and standard control injected MOs. Only 1.4% blastocyst formation rates were observed with the Msk2 MO-injected one-cell mouse embryos (Fig. 4B and Table 1) and co-injection with a modified *Msk2* mRNA designed to avoid direct targeting of the Msk2 morpholino (Supplementary Fig. S5a and b) partially rescued this defect by significantly increasing blastocyst development to ∼36% ($P < 0.001$). Notably, of the ∼75 mouse embryos injected with the Msk2 MO, only a single embryo developed to the blastocyst stage (Fig. 4C and Table 1). This exception may be due to minor differences in the volume of MO injected into each embryo as demonstrated by the slight variation in fluorescent intensities between embryos following sequential injection (Fig. 4D). However, we observed that there was a decrease in the expression of Msk2 detected in the one Msk2 MO-injected embryo that reached the blastocyst stage compared with the level of Msk2 expression detected in non-injected, water or 3′-carboxyfluorescein-labeled MO-injected embryos (Fig. 4E).

Following our observation that the knockdown of Msk2 in mouse embryos significantly reduced blastocyst formation rates, we then examined the developmental timing of embryo arrest. A closer examination of each stage of pre-implantation development revealed that Msk2-mediated arrest most commonly occurred in three- to eight-cell embryos (Fig. 5A). More specifically, arrest was observed in ∼40% of three- to four-cell embryos and 51% of six- to eight-cell embryos following injection of the Msk2 MO ($P < 0.001$; Fig. 5B). In addition, we also determined that the few embryos that arrested at the one-cell stage was due to polyploidy (Fig. 5C; upper panel) and that a decrease in Msk2 expression was observed in non-polyploid Msk2 MO-injected two-cell mouse embryos prior to arrest in comparison with 3′-carboxyfluorescein-labeled MO-injected embryos at a similar stage (Fig. 5C; middle and lower

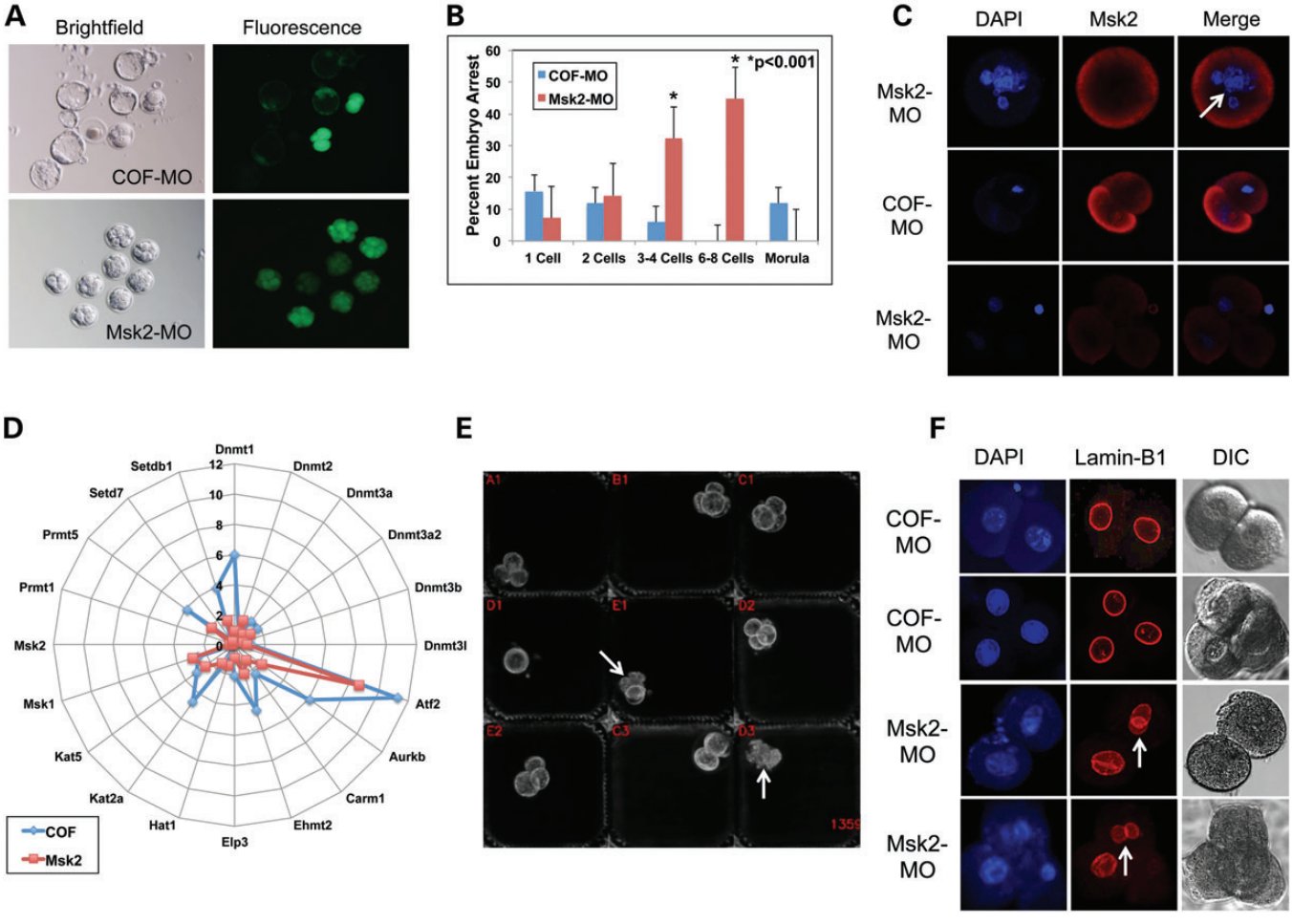

Figure 5. Msk2 knockdown induces mitotic arrest and is associated with aneuploidy generation. (**A**) Brighfield imaging and fluorescent microscopy of 3′-carboxyfluorescein-labeled standard control morpholino (COF-MO) and Msk2 morpholino (Msk2 MO)-injected mouse embryos demonstrates that the Msk2 MO-mediated embryonic arrest occurs at the cleavage stage. (**B**) A closer examination of each developmental stage reveals a significant increase ($P < 0.001$) in Msk2 MO-induced arrest at the three- to eight-cell stages. (**C**) Confocal microscopy of Msk2 expression in DAPI stained embryos shows that the embryo arrest that occurred at the one-cell stage following Msk2 MO injection is due to other reasons such as polyploidy (indicated by white arrow) and that reduced Msk2 expression is observed in Msk2 MO compared with COF-MO-injected embryos. (**D**) Gene expression analysis of DNMTs and histone-modifying enzymes in COF-MO and Msk2 MO-injected embryos demonstrates that Msk2 knockdown has effects on other known mitotic regulators. (**E**) The last frame of an image sequence compiled into a time-lapse movie (Supplementary Material, Movie S3), which shows increased blastomere movement and eventual lysis resembling mitotic catastrophe in some Msk2 MO-injected embryos. (**F**) Lamin-B1-encapsulated micronuclei are observed in Msk2 MO, but not COF-MO-injected embryos stained with DAPI and imaged by DIC ($n = 10$ embryos from each group), suggesting that mouse embryos may avoid chromosomal instability by inducing cell lysis.

panels). Finally, when we evaluated the epigenetic expression profiles in 3′-carboxyfluorescein-labeled MO- or Msk2 MO-injected embryos, we detected considerably lower expression levels of *Dnmt1* and *Aurkb*, additional epigenetic regulators that have known mitotic functions (45,46), in Msk2 MO embryos (Fig. 5D), suggesting that Msk2 knockdown had adverse effects on other epigenetic mediators in developing embryos. Assessment of embryo behavior by time-lapse imaging also revealed that Msk2 MO-injected embryos exhibited the unusual phenotype of increased internal blastomere movement and lysis upon arrest (Fig. 5E and Supplementary Material, Movie S3), which was not observed in *Msk2* mRNA rescued blastocysts (Supplementary Material, Movie S4). We note that this phenotype resembled the aberrant mitosis and cell death observed during mitotic catastrophe (47) and reasoned that perhaps the lysis of blastomeres induced by Msk2-mediated knockdown may constitute a mechanism for mouse embryos to avoid chromosomal instability. In support of this, we immunostained mouse embryos with Lamin-B1, a nuclear envelope marker, and observed the formation of Lamin-B1 encapsulated micronuclei in Msk2 MO-injected, but not 3′COF MO-injected embryos prior to lysis (Fig. 5F).

Association between MSK2 expression, mitosis and aneuploidy in human embryos

Given our findings that the embryo arrest in Msk2 MO-injected embryos was associated with mitotic arrest and micronucleation, our next aim was to determine whether *MSK2* was involved in abnormal mitotic divisions and possible aneuploidy generation in human embryos. Our experimental design for this is as shown in Figure 1B and made use of previous studies. By measuring previously identified cell cycle parameters predictive of blastocyst formation prior to EGA (1), we recently demonstrated

Table 1. The number and percentage of blastocysts obtained in independent microinjection experiments

	Non-injected (NI)	Water-injected (DW)	3′-Carboxyfluorescein morpholino-injected (COF)	Msk2 morpholino-injected (Msk2 MO)	Msk2 morpholino + modified mRNA-injected (Msk2 MO + mRNA)
Number of independent experiments	7	2	7	7	3
Number of embryos reaching blastocyst stage	61	15	55	1	12
Total number of embryos	73	19	71	73	33
Percentage	83	79	77	1.4	36

A table displaying the number of independent experiments performed, the number of embryos that reached the blastocyst stage out of the total number of embryos with the corresponding percentage in the different microinjection groups. Note that only one embryo became a blastocyst in the Msk2 MO-injected group and this Msk2-induced embryo arrest was partially rescued by co-injecting with a similar concentration (20 ng/μl) of modified Msk2 mRNA (Msk2 MO + mRNA). This table is an accompaniment to Figure 4B.

that blastomere behavior reflects human embryo ploidy by the four-cell stage (5) and that chromosome-containing micronuclei/fragments may contribute to the complex aneuploidy observed in cleavage-stage human embryos (5,48,49). Therefore, we similarly analyzed cell cycle parameter timing in human embryos cultured from the zygote to approximately the four-cell stage using time-lapse imaging and evaluated each embryo for the expression of MSK2 and LAMIN-B1 (Fig. 1B). We detected significantly lower MSK2 expression in blastomeres with visible micronuclei and abnormal cell cycle parameters, whereas high MSK2 expression was observed in blastomeres with intact primary nuclei and normal parameter timing (Fig. 6A and Supplementary Material, Fig. S6; $P < 0.01$). In those embryos with micronuclei, we also observed a lack of both H3-S10 and H3-S28 phosphorylation, two of the histone modifications that MSK2 mediates (50,51), but not H4-K16 acetylation, which has been shown to be involved in DNA repair and programmed cell death (52) (Fig. 6B). Thus, the absence of MSK2 expression and its corresponding histone modifications appears to be related to both abnormal mitotic divisions and micronuclei formation and may potentially contribute to aneuploidy generation in human embryos.

To further investigate the role of *MSK2* in human preimplantation development, we analyzed the expression of both full-length *MSK2* (MSK2-2) as well an alternative *MSK2* splice variant (MSK2-1; Supplementary Material, Table S2), which does not exist in the mouse (53), in single blastomeres from cleavage-stage embryos that were determined to be either euploid (Supplementary Material, Fig. S7a) or aneuploid (Supplementary Material, Fig. S7b) by array-comparative genomic hybridization (A-CGH). While both *MSK2* isoforms were more highly expressed in the blastomeres of euploid embryos ($n = 13$), low to moderate levels of *MSK2* expression were detected in aneuploid embryos ($n = 20$) to support a role for *MSK2* in regulating human embryonic aneuploidy generation (Fig. 6C). Given that between 50 and 80% of cleavage-stage human embryos are chromosomally abnormal (5,48,49), this may also help explain why *MSK2* expression was only detected in a few blastomeres from human embryos at the eight-cell stage (Fig. 2D). In addition, *DNMT1*, *AURKA* and *AURKB*, but not *MSK1* were also expressed in a similar pattern as *MSK2* expression in euploid and aneuploid embryos to suggest an association between *MSK2*, *DNMT1*, *AURKA* and *AURKB* function.

Growth factor supplementation restores epigenetic expression levels in human embryos

Based on previous studies suggesting that media supplementation of certain autocrine/paracrine factors can enhance oocyte maturation and early embryo development (54,55), our final objective was to determine whether the addition of defined growth factors to culture media had any effects on the expression of epigenetic regulators in human embryos by Q-PCR (Fig. 1B). For this purpose, we evaluated DNMT and histone-modifying enzyme expression in embryos cultured with a growth factor cocktail containing brain-derived neurotrophic factor (BDNF), insulin-like growth factor 1 (IGF-I), epidermal growth factor (EGF), granulocyte macrophage colony-stimulating factor (GM-CSF), basic fibroblast growth factor (bFGF)/FGF2 and glial cell line-derived neurotrophic factor (GDNF), which were selected based on the aforementioned studies (54,55) as well as the confirmation of their corresponding receptor expression in human oocytes (56). Although similar blastocyst formation rates (∼30%) were observed with human zygotes cultured in the absence or presence of the growth factor cocktail, comparison of gene expression between the two groups revealed that media supplementation induced changes in DNMT and histone-modifying enzyme expression beginning at the eight-cell stage (Supplementary Material, Fig. S8). Analysis of epigenetic regulator expression in blastocysts from both fertile and infertile patients also revealed differences in DNMT and histone-modifying enzyme expression levels (Fig. 6D). More importantly, when epigenetic regulator expression was compared in infertile, fertile and growth factor treated blastocysts, we determined that media supplementation either partially or fully restored the expression levels of several DNMTs and histone-modifying enzymes, including *MSK2*, to that observed in embryos from fertile patients (Fig. 6D). Thus, our data suggest that the addition of growth media may potentially reduce chromosomal instability and improve IVF outcomes by positively influencing the expression of epigenetic regulators in human embryos.

DISCUSSION

To our knowledge, this is the first study to directly compare DNA methylation and histone modification patterns in both the mouse and human, individual embryos and single cells, at the mRNA as

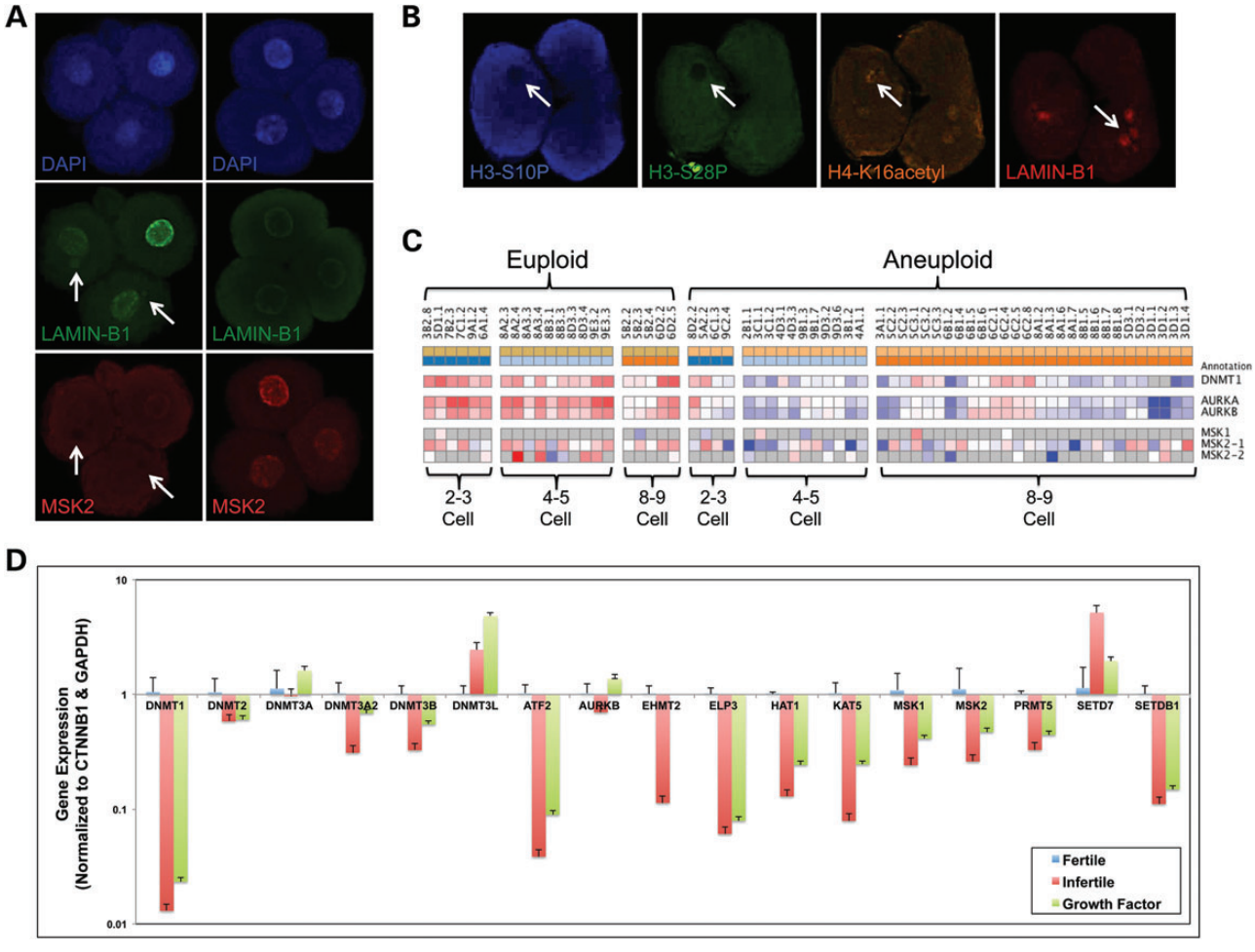

Figure 6. Association between mitosis, aneuploidy and the expression of epigenetic regulators in human embryos. (**A**) Human zygotes were cultured until the four-cell stage and previously identified cell cycle parameters predictive of blastocyst formation and ploidy status were measured by time-lapse image analysis. Embryos with abnormal parameter timing and micronuclei exhibited low MSK2 expression, whereas high MSK2 expression was observed in embryos with intact primary nuclei and normal parameter timing as quantified in Supplementary Material, Figure S6. (**B**) A lack of both H3-S10P and H3-S28P, two of the histone modifications that MSK2 mediates, was also observed in embryos with micronuclei in contrast to elevated H4-K16acetyl, which has been shown to be involved in DNA repair and apoptosis. (**C**) Gene expression analysis of cleavage-stage human embryos determined to be euploid or aneuploid by A-CGH as shown in Supplementary Material, Figure S7. Note the high levels of expression of both *MSK2* isoforms, *DNMT1*, *AURKA* and *AURKB,* but not *MSK1* in euploid embryos ($n = 13$) compared with aneuploid embryos ($n = 20$). Grey squares indicate no expression, whereas blue, white and red squares correspond to low, medium and high expression, respectively. (**D**) Comparison of DNMT and histone-modifying enzyme expression in fertile, infertile and GFC-treated blastocysts ($n = 6–8$ embryos from each group) by Q-PCR demonstrates that growth factor supplementation can partially restore the expression of epigenetic regulators to levels observed in embryos from fertile patients and beginning at the eight-cell stage of development as demonstrated in Supplementary Material, Figure S8.

well as protein level, in embryos from fertile and infertile couples and following growth factor supplementation. In addition, we further interrogated the function of a particular epigenetic regulator in mouse and human pre-implantation development. While DNMT expression patterns differed substantially between mouse and human embryos, mRNA expression levels and timing of the histone-modifying enzymes, *ATF2*, *KAT5*, *MSK2*, *PRMT5* and *SETDB1* were similar in these two species. Since both *ATF2* and *KAT5* are involved in the acetylation of lysine residues, *MSK2* in the phosphorylation of serine residues, *PRMT5* in the methylation of arginine residues and *SETDB1* in the methylation of lysine residues (50,51,57–60), this suggests that expression of at least one member from each histone-modifying enzyme class is conserved between human and mouse development (Fig. 7). There also remains the possibility that homologous DNMT genes with analogous functions could be similarly expressed between mouse and human embryos (61–63).

The greatest variation in DNMT, histone modification and histone-modifying enzyme expression was observed between human embryos beginning at the four- to eight-cell stages, which we attributed, at least in part, to differences between single cells within the same embryo. We previously demonstrated by single-cell gene expression profiling that human blastomeres develop cell autonomously (1) and this is supported by the findings presented here since we show that individual blastomeres within the human embryo can simultaneously express different epigenetic marks. Given that some of these epigenetic marks are differentially associated with mitosis, DNA repair and transcriptional activation and/or silencing (33,34,51,52),

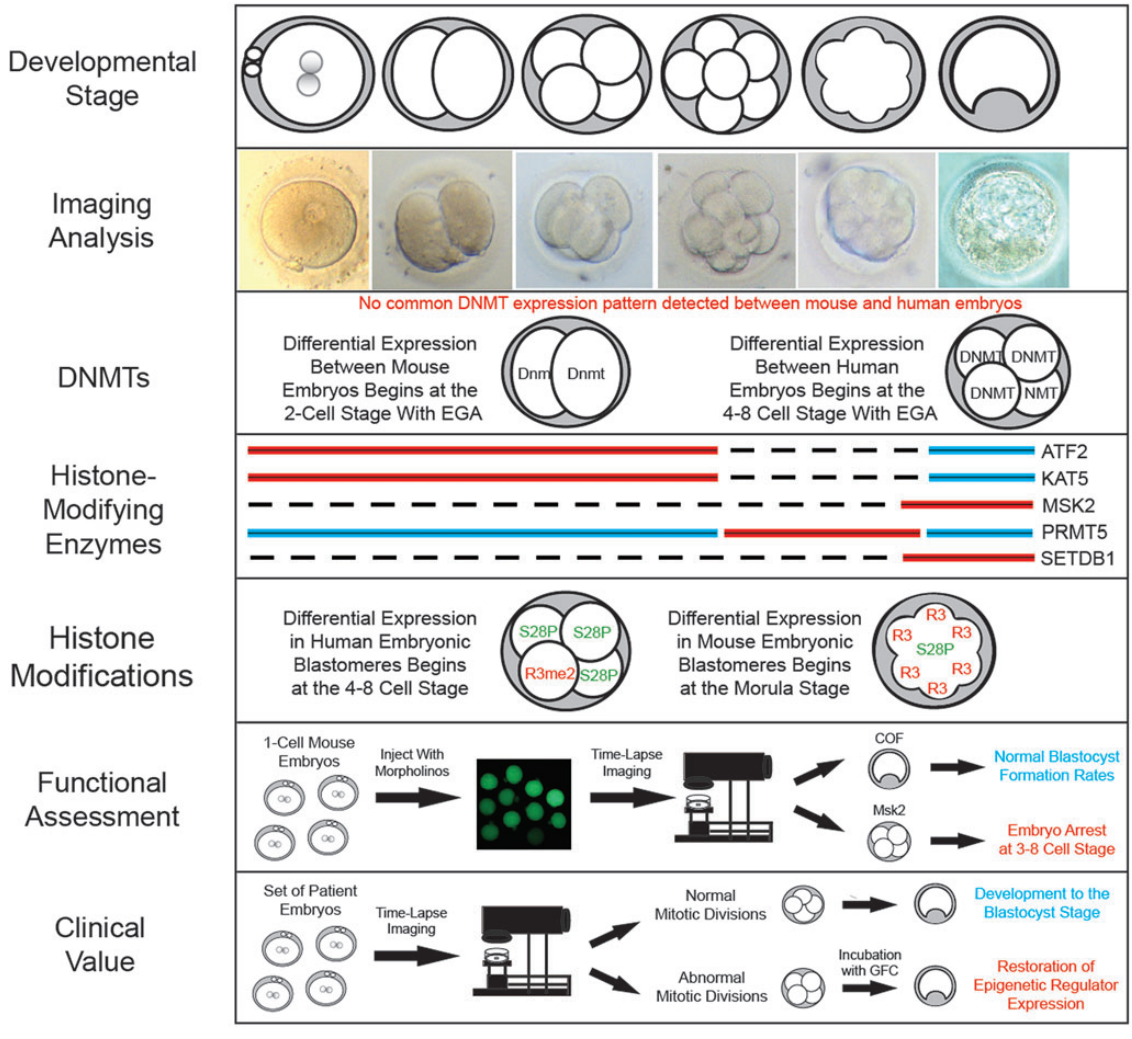

Figure 7. Summary model of epigenetic regulation during pre-implantation development. Embryonic development was monitored in both mouse and human embryos by imaging analysis from the zygote to the blastocyst stage. While no common DNMT expression pattern was detected, we did observe similar gene expression profiles for *ATF2*, *KAT5*, *MSK2*, *PRMT5* and *SETDB1* between mouse and human embryos, which was determined to be due, in part, to differences in expression at the single-cell level and coincided with the timing of EGA in each species. We also observed differences in the sub-compartmentalization of particular histone modifications between blastomeres in the same embryo of the two species; in humans, this occurred at the four- to eight-cell stages, while mice exhibited differential blastomere expression beginning at the morula stage. The function of the histone-modifying enzyme, *Msk2*, was further assessed by morpholino technologies and determined to induce micronuclei formation, embryo arrest and eventual blastomere lysis at the three- to eight-cell stages. Correlations to human embryonic development were made by observing low MSK2 expression in human embryos with aneuploidy, micronuclei and aberrant mitotic divisions. Based on the restoration of epigenetic regulator expression in infertile patient embryos incubated with a growth factor cocktail (GFC), we also suggest the clinical value of GFC addition to those embryos with abnormal cell cycle parameters subjected to prolonged culture.

findings also support the concept that blastomeres of the human embryo may have divergent developmental potential beginning at the four- to eight-cell stages (Fig. 7). Given the extension of epigenetics to microRNAs (miRNAs) and our previous findings of distinct differences in the expression of miRNA biogenesis genes in normal versus arrested one-cell and two-cell human embryos (1) and normal versus parthenogenetic morulas and blastocysts (56), the likely importance of epigenetic-miRNA regulation beyond the two-cell stage and especially in the context of aneuploidy should be further investigated.

In order to functionally validate our findings, we reduced expression of the histone-modifying enzyme, Msk2, and examined the effects in the mouse for potential correlation to human pre-implantation development. Although knockout mice for *Msk2* are reported to be viable and fertile, it is not clear whether this conclusion was drawn from heterozygous or homozygous crosses as these details are not provided in the study (50). Moreover, we suspect that we observed such a profound phenotype in our study since the Msk2 morpholino may potentially target all Msk2 mRNAs whether embryonic, maternally or paternally derived, the latter of which may be associated with hypomethylation and histone-retained regions in sperm (64,65). Nonetheless, another study has shown that *Msk1/Msk2* double knockout mice exhibit hypersentivity to endotoxins and prolonged inflammation (66) and thus, it will be important to assess fecundity in Msk1 and/or Msk2 mouse knockouts generated by site-specific enginneered nucleases (67,68) or in specific cells and tissues using conditional Msk2 knockout mice (69).

Following injection of the Msk2 MO in one-cell embryos here, we observed almost complete embryo arrest at the three- to eight-cell stage and an unusual phenotype in which increased cell movement and eventual blastomere lysis was detected. Based on the observations that reduced Msk2 expression had effects on the expression of *Dnmt1* and *Aurkb*, both of which are known to have important roles in mitosis and possibly ploidy status (45,46,70), this suggests that the embryo arrest observed after Msk2 injection is likely due to a defect in mitosis. In addition, we further suggest that the blastomere lysis observed following Msk2 MO injection resembles cellular events described during mitotic catastrophe (47), may represent a mechanism for embryos to avoid chromosomal instability and explain the low aneuploidy rates observed in mice (71). A correlation between *MSK2* expression and human aneuploidy generation is supported by our findings of abnormal cell cycle parameter timing, ploidy status, micronuclei formation, reduced MSK2 expression and alterations in histone modifications mediated by MSK2, in human embryos (Fig. 7), the latter of which has similar indications in lower organisms (72). Whether low MSK2 expression is a cause or consequence of aneuploidy is unknown, but based on previous findings of a prolonged G1 phase in MSK2-deficient cells (44) and that a closely related family member is a kinetochore-associated protein that participates in the spindle assembly checkpoint (73), it is likely that reduced MSK2 expression prevents the localization and function of several proteins involved in cell cycle progression. Thus, further investigation is required to determine whether *MSK2* prevents aneuploidy generation directly or indirectly via *DNMT1*, *AURKA*/*AURKB* and/or other cell cycle associated genes and the exact mechanism by which *MSK2* mediates its function.

Finally, while we did observe differences in epigenetic expression profiles between fertile and infertile patient embryos, the incubation of embryos from infertile couples with a growth factor cocktail either partially or fully restored the expression levels of numerous epigenetic factors beginning at the eight-cell stage when the major wave of EGA occurs (3,26). This suggests that the addition of select growth factors to embryo culture media may prevent alterations in epigenetic profiles (Fig. 7) and potentially improve developmental competence of patient embryos subjected to prolonged culture. Altogether, our data suggest that although epigenetic mechanisms do not alter DNA sequence, they may have essential roles for pre-implantation development and possible pregnancy outcomes, especially in the context of IVF. There may also be more long-term implications of these findings, including an association with the fetal origins of adult disease and transgenerational inheritance of epigenetic changes or defects. The work described here contributes to our understanding of the epigenetic requirements for normal embryogenesis, in cases of human reproductive failure, and may be applied to clinical improvement of assisted reproduction.

MATERIALS AND METHODS

Sample source and procurement

Approximately 150 supernumerary human embryos subsequently donated for non-stem research were obtained with written informed consent from the Stanford University Regenerative Medicine through the Ethical procurement of Nonviable or Excess cellular Waste (RENEW) Biobank and the Reproductive Medicine Center at the University of Minnesota, which received embryos from the Lutheran General Hospital IVF Program (Park Ridge, IL, USA) when it closed in 2002. De-identification and molecular analysis was performed according to the Stanford University Institutional Review Board (IRB)-approved protocol #10466 entitled 'The RENEW Biobank' (74) and the University of Minnesota IRB-approved protocol #0306M49242 entitled 'Stage-Specific Genomic Characterization of Human Pre-implantation Embryos'. No protected health information was associated with each of the embryos. The average maternal age was 34 years old and the most common cause of infertility was unexplained at 35% of couples. Embryos from patients classified as fertile was based on the use of donor materials for IVF cycles and the inclusion of embryos from fertile couples seeking gender selection or Human Leukocyte Antigen (HLA) typing.

Human embryo thawing and culture

Human embryos were thawed by a two-step rapid thawing protocol using Quinn's Advantage Thaw Kit (CooperSurgical, Trumbull, CT, USA) as previously described (1,5). In brief, either cryostraws or vials were removed from the liquid nitrogen and exposed to air before incubating in a 37°C water bath. Once thawed, embryos were transferred to a 20 μl microdrop of either Quinn's Advantage Cleavage Medium (CooperSurgical) supplemented with 10% SPS between Days 1–3 or Quinn's Advantage Blastocyst Medium (CooperSurgical) with 10% SPS after Day 3 under mineral oil (Sigma, St Louis, MO, USA). Approximately half of the embryos were also cultured in the presence of a growth factor cocktail containing 10 ng/ml BDNF (PeptroTech Inc., Rocky Hill, NJ, USA), 40 ng/ml IGF-I (Sigma-Aldrich, St Louis, MO, USA), 5 ng/ml EGF (R&D Systems, Inc., Minneapolis, MN, USA), 2 ng/ml GM-CSF (R&D Systems, Inc.), 0.5 ng/ml FGF2 (R&D Systems, Inc.) and 10 ng/ml of GDNF (R&D Systems, Inc.). All embryos were cultured at 37°C with 6% CO_2, 5% O_2 and 89% N_2 and embryo development was monitored daily by microscope for up to 7 days.

Mouse embryo collection and culture

Three- to five-week-old wild-type C57BL6 × DBA/2 (B6D2F1) female F1 mice were obtained from Charles River (Hollister, CA, USA) and superovulated by intraperitonial injections of 10 IU of Pregnant Mare's Serum Gonadotropin (PMSG; Sigma) followed by 10 IU of human Chorionic Gonadotropin (hCG; Sigma) 48 h later and mated overnight with wild-type B6D2F1 male mice. Females were sacrificed by cervical dislocation ∼18 h after hCG injection and their oviducts, along with the adjacent uterine and ovarian tissue, were removed and transferred to EmbryoMax M2 Medium (Millipore, Billerica, MA, USA) for dissection. One-cell embryos were released from the oviducts and cumulus cells were removed from the embryos by hyaluronidase (Sigma) treatment and gentle pipetting. Two pronuclei stage embryos were recovered, pooled from 8 to 10 females in M2 media and similarly cultured in Quinn's Advantage Cleavage Medium with 10% SPS at 10 embryos per 20 μl microdrop. All procedures involving animals were performed under the Institutional Animal Care and Use Committee

(IACUC) protocol #16146 entitled 'Molecular Analysis of Embryogenesis and Gametogenesis,' which was approved by the Administrative Panel on Laboratory Animal Care (APLAC) at Stanford University.

Single embryo and cell gene expression analysis

Gene expression was analyzed in mouse and human embryos using the BioMark Dynamic Array microfluidic system (Fluidigm Corp., So. San Francisco, CA, USA). The zona pellucida (ZP) was removed by treatment with Acidified Tyrode's Solution (Millipore) and ZP-free embryos were washed in Quinn's Advantage Medium with Hepes plus 5% SPS three times and then quick frozen in phosphate buffered solution (PBS; Invitrogen, Carlsbad) with 0.1% bovine serum albumin (BSA; Sigma-Aldrich) on dry ice for storage at −80°C until use. Cleavage-stage human embryos were dissembled to single cells in Quinns Advantage Medium with HEPES (Ca and Mg Free; Copper Surgical) plus 10% Human Albumin (Cooper Surgical), while mouse embryos were dissembled in 0.25% trypsin-EDTA (Gibco) plus 10% human albumin both at 37°C with gentle pipetting. Individual embryos and single cells were pre-amplified according to the manufacturer's protocol (Fluidigm Corp.) using the CellsDirect One-Step qRT-PCR kit (Invitrogen) and 20× TaqMan gene expression assays (Applied Biosystems, Foster City, CA, USA) or gene-specific primers designed to span exons using Primer-BLAST (NCBI). Pre-amplified cDNA was loaded into the sample inlets of a 96 × 96 dynamic array (DA; Fluidigm Corp.) and assayed in triplicate. The expression of between 6 and 10 housekeeping genes was analyzed as a control. Calculated normalized relative quantity (CNRQ) values were calculated and normalized to the two or three most stable housekeeping genes using the qBasePlus 1.3 analysis software (http://www.biogazelle.com) as previously described (75) and graphed using Gene-E (http://www.broadinstitute.org/cancer/software/GENE-E/).

Antibodies

The Histone H3-S10P mouse monoclonal antibody (clone 6G3) was purchased from Cell Signaling Technology, Inc. (Danvers, MA, USA), whereas the H3-S28P rat monoclonal (clone HTA28) and the H4-R3me2 rabbit polyclonal antibody (catalog #39275) were obtained from Thermo Fisher Scientific (Rockford, IL, USA) and Active Motif (Carlsbad, CA, USA), respectively. The Histone H3-K4me3 rabbit monoclonal antibody (clone MC315) was purchased from Millipore, while the Histone H4-K16acetyl goat polyclonal antibody (catalog #sc-8662) was obtained from Santa Cruz Biotechnology, Inc. (Santa Cruz, CA, USA). The Msk2 rabbit polyclonal (catalog # ab42282), Lamin-B1 rabbit polyclonal (catalog #ab16048) and Gapdh rabbit polyclonal (catalog #ab9485) antibodies were obtained from Abcam (Cambridge, MA, USA).

The Alexa Fluor donkey anti-mouse 405 antibody (custom synthesis), donkey anti-rat 488, donkey anti-sheep 488, donkey anti-goat 568 and donkey anti-rabbit 647 antibodies were purchased from Invitrogen (Carlsbad, CA, USA) for confocal imaging analysis. As controls, the mouse, rat, rabbit and goat IgG isotype antibodies were obtained from Vector Laboratories (Burlingame, CA, USA).

Confocal imaging analysis and three-dimensional modeling

ZP-free mouse and human embryos were obtained as described above and washed in PBS plus 0.1% BSA and 0.1% Tween-20 (PBS-T; Sigma-Aldrich) before fixation in either 100% cold methanol for 20 min at −20°C to avoid DNA-histone crosslinking or 4% paraformaldehyde in PBS (USB Corp., Cleveland, OH, USA) for 20 min at room temperature (RT) when visualizing non-histone associated proteins. Once fixed, the embryos were washed three times in PBS-T to remove any residual fixative and permeabilized in 1% Triton X-100 (Sigma-Aldrich) for 1–2 h at RT. Following permeabilization, the embryos were washed three times in PBS-T and then blocked in 4% normal donkey serum (Jackson ImmunoReasearch Laboratories, Inc., West Grove, PA, USA) in PBS-T overnight at 4°C. The embryos were incubated with primary antibodies in PBS-T with 1% donkey serum sequentially for 1 h each at RT at the following dilutions: mouse H3-S10P (1:200), rat H3-S28P (1:200), rabbit H4-R3me2 (1:1000), rabbit H3-K4me3 (1:200) and goat H4-K16Ac (1:200) and/or with rabbit Msk2 (1:400) and Lamin-B1 (1:1000). Primary signals were detected using the appropriate 405, 488, 568 or 647 conjugated donkey Alexa Fluor secondary antibody (Invitrogen) at a 1:250 dilution at RT for 1 h in the dark. Immunofluorescence was visualized by sequential imaging, whereby the channel track was switched each frame to avoid cross-contamination between channels, using a Zeiss LSM510 Meta inverted laser scanning confocal microscope described here: http://nisms.stanford.edu/Equipment/LSM510Meta01v01.html. The instrument settings, including the laser power, pinhole and gain, were kept constant for each channel to facilitate semi-quantitative comparisons between developmental stages and mouse and human embryos. Confocal sections were captured at 1 mm intervals throughout the whole embryo and processed in ImageJ (NIH) for Z-stack imaging analysis. Three-dimensional reconstructions of embryos were accomplished with IMARIS (Bitplane). Semi-quantitative analysis of MSK2 expression in human embryos was performed by measuring the mean pixel intensity of immunostaining in each blastomere using ImageJ.

Microinjection of antisense MOs

Initial concentrations of 0.05–0.6 mM of 3′-carboxyfluorescein-labeled morpholino were injected into mouse zygotes based on previous findings (76) and it was determined that 0.3 mM of the standard control was the maximum concentration that would allow normal rates of blastocyst development. Therefore, a similar concentration of Msk2 morpholino with the sequence 5′-CCTCGTCCTCATCCTCGTCTCCCAT-3′, which was designed to target the translation start site of Msk2 and labeled with 3′-carboxyfluorescein for visualization, was injected into the cytoplasm of each embryo using a CellTram vario (Eppendorf, Hauppauge, New York, USA), electronic microinjector (Narashige IM300, Japan) and Transferman NK 2 Micromanipulator (Eppendorf). Non-injected, water-injected and the injection of a 3′-carboxyfluorescein-labeled standard control MO that does not target any known sequence in the mouse genome or transcriptome served as controls in each experiment to assess enzyme-MO-mediated knockdown. Each MO was prepared in water and incubated at 65°C for 10 min prior to injection.

Statistical analysis

The data are represented as the average ± the standard deviation and analyzed for statistical significance ($P < 0.05$) using the one-way ANOVA with the Bonferonni correction. All experiments were repeated at least three times with similar results.

AUTHORS' CONTRIBUTIONS

S.L.C. designed and performed experiments, analyzed data, wrote and edited the manuscript. S.L.M. performed experiments, analyzed data and wrote and edited the manuscript. N.L.B., M.V.R., D.E.L. and B.B. performed experiments and assisted in the writing and editing of the manuscript. C.J.D. and L.M.W. interpreted results and assisted in the writing and editing of the manuscript. R.A.R.P. assisted in the design of experiments, interpreted results and assisted in the writing and editing of the manuscript.

SUPPLEMENTARY MATERIAL

Supplementary Material is available at *HMG* online.

ACKNOWLEDGEMENTS

The authors gratefully acknowledge Tasha Kalista, H. Austinn Freeman, Tracy Lindsay and Dharti Trivedi who managed the Stanford RENEW bank. We also thank Drs Yimin Shu, Kevin Loewke, Jinnuo Han, Connie Wong and Andrew Olson as well as Akshi Goyal, Jens Durruthy-Durruthy, Bahareh Haddad Derafshi and Ha Nam Nguyen for technical assistance with these studies.

Conflict of Interest statement. None declared.

FUNDING

This work was supported, in part, by the California Institute for Regenerative Medicine (CIRM; RB3-02209 to R.A.R.P.) and a grant from the March of Dimes (6-FY10-351 to R.A.R.P.). Funding to pay the Open Access Publications Charges was provided by private funds.

REFERENCES

1. Wong, C.C., Loewke, K.E., Bossert, N.L., Behr, B., De Jonge, C.J., Baer, T.M. and Reijo Pera, R.A. (2010) Non-invasive imaging of human embryos before embryonic genome activation predicts development to the blastocyst stage. *Nat. Biotechnol.*, **28**, 1115–1121.
2. Wossidlo, M., Nakamura, T., Lepikhov, K., Marques, C.J., Zakhartchenko, V., Boiani, M., Arand, J., Nakano, T., Reik, W. and Walter, J. (2011) 5-Hydroxymethylcytosine in the mammalian zygote is linked with epigenetic reprogramming. *Nat. Commun.*, **2**, 241.
3. Vassena, R., Boue, S., Gonzalez-Roca, E., Aran, B., Auer, H., Veiga, A. and Izpisua Belmonte, J.C. (2011) Waves of early transcriptional activation and pluripotency program initiation during human preimplantation development. *Development*, **138**, 3699–3709.
4. Plachta, N., Bollenbach, T., Pease, S., Fraser, S.E. and Pantazis, P. (2011) Oct4 kinetics predict cell lineage patterning in the early mammalian embryo. *Nat. Cell Biol.*, **13**, 117–123.
5. Chavez, S.L., Loewke, K.E., Han, J., Moussavi, F., Colls, P., Munne, S., Behr, B. and Reijo Pera, R.A. (2012) Dynamic blastomere behaviour reflects human embryo ploidy by the four-cell stage. *Nat. Commun.*, **3**, 1251.
6. Xue, Z., Huang, K., Cai, C., Cai, L., Jiang, C.Y., Feng, Y., Liu, Z., Zeng, Q., Cheng, L., Sun, Y.E. *et al.* (2013) Genetic programs in human and mouse early embryos revealed by single-cell RNA sequencing. *Nature*, **500**, 593–597.
7. Kafri, T., Ariel, M., Brandeis, M., Shemer, R., Urven, L., McCarrey, J., Cedar, H. and Razin, A. (1992) Developmental pattern of gene-specific DNA methylation in the mouse embryo and germ line. *Genes Dev.*, **6**, 705–714.
8. Reik, W. (2007) Stability and flexibility of epigenetic gene regulation in mammalian development. *Nature*, **447**, 425–432.
9. Lewis, J.D., Meehan, R.R., Henzel, W.J., Maurer-Fogy, I., Jeppesen, P., Klein, F. and Bird, A. (1992) Purification, sequence, and cellular localization of a novel chromosomal protein that binds to methylated DNA. *Cell*, **69**, 905–914.
10. Nan, X., Ng, H.H., Johnson, C.A., Laherty, C.D., Turner, B.M., Eisenman, R.N. and Bird, A. (1998) Transcriptional repression by the methyl-CpG-binding protein MeCP2 involves a histone deacetylase complex. *Nature*, **393**, 386–389.
11. Jones, P.L., Veenstra, G.J., Wade, P.A., Vermaak, D., Kass, S.U., Landsberger, N., Strouboulis, J. and Wolffe, A.P. (1998) Methylated DNA and MeCP2 recruit histone deacetylase to repress transcription. *Nat. Genet.*, **19**, 187–191.
12. Robert, M.F., Morin, S., Beaulieu, N., Gauthier, F., Chute, I.C., Barsalou, A. and MacLeod, A.R. (2003) DNMT1 is required to maintain CpG methylation and aberrant gene silencing in human cancer cells. *Nat. Genet.*, **33**, 61–65.
13. May, A., Kirchner, R., Muller, H., Hartmann, P., El Hajj, N., Tresch, A., Zechner, U., Mann, W. and Haaf, T. (2009) Multiplex rt-PCR expression analysis of developmentally important genes in individual mouse preimplantation embryos and blastomeres. *Biol. Reprod.*, **80**, 194–202.
14. Golding, M.C. and Westhusin, M.E. (2003) Analysis of DNA (cytosine 5) methyltransferase mRNA sequence and expression in bovine preimplantation embryos, fetal and adult tissues. *Gene Expr. Patterns*, **3**, 551–558.
15. Vassena, R., Dee Schramm, R. and Latham, K.E. (2005) Species-dependent expression patterns of DNA methyltransferase genes in mammalian oocytes and preimplantation embryos. *Mol. Reprod. Dev.*, **72**, 430–436.
16. Huntriss, J., Hinkins, M., Oliver, B., Harris, S.E., Beazley, J.C., Rutherford, A.J., Gosden, R.G., Lanzendorf, S.E. and Picton, H.M. (2004) Expression of mRNAs for DNA methyltransferases and methyl-CpG-binding proteins in the human female germ line, preimplantation embryos, and embryonic stem cells. *Mol. Reprod. Dev.*, **67**, 323–336.
17. Latham, J.A. and Dent, S.Y. (2007) Cross-regulation of histone modifications. *Nat. Struct. Mol. Biol.*, **14**, 1017–1024.
18. Liu, H., Kim, J.M. and Aoki, F. (2004) Regulation of histone H3 lysine 9 methylation in oocytes and early pre-implantation embryos. *Development*, **131**, 2269–2280.
19. Torres-Padilla, M.E., Parfitt, D.E., Kouzarides, T. and Zernicka-Goetz, M. (2007) Histone arginine methylation regulates pluripotency in the early mouse embryo. *Nature*, **445**, 214–218.
20. Qiao, J., Chen, Y., Yan, L.Y., Yan, J., Liu, P. and Sun, Q.Y. (2010) Changes in histone methylation during human oocyte maturation and IVF- or ICSI-derived embryo development. *Fertil. Steril.*, **93**, 1628–1636.
21. Sarmento, O.F., Digilio, L.C., Wang, Y., Perlin, J., Herr, J.C., Allis, C.D. and Coonrod, S.A. (2004) Dynamic alterations of specific histone modifications during early murine development. *J. Cell Sci.*, **117**, 4449–4459.
22. Veeck, L.L., Amundson, C.H., Brothman, L.J., DeSciscIolo, C., Maloney, M.K., Muasher, S.J. and Jones, H.W. Jr (1993) Significantly enhanced pregnancy rates per cycle through cryopreservation and thaw of pronuclear stage oocytes. *Fertil. Steril.*, **59**, 1202–1207.
23. Miller, K.F. and Goldberg, J.M. (1995) In vitro development and implantation rates of fresh and cryopreserved sibling zygotes. *Obstet. Gynecol.*, **85**, 999–1002.
24. El-Toukhy, T., Khalaf, Y., Al-Darazi, K., O'Mahony, F., Wharf, E., Taylor, A. and Braude, P. (2003) Cryo-thawed embryos obtained from conception cycles have double the implantation and pregnancy potential of those from unsuccessful cycles. *Hum. Reprod.*, **18**, 1313–1318.
25. Flach, G., Johnson, M.H., Braude, P.R., Taylor, R.A. and Bolton, V.N. (1982) The transition from maternal to embryonic control in the 2-cell mouse embryo. *EMBO J.*, **1**, 681–686.
26. Dobson, A.T., Raja, R., Abeyta, M.J., Taylor, T., Shen, S., Haqq, C. and Pera, R.A. (2004) The unique transcriptome through day 3 of human preimplantation development. *Hum. Mol. Genet.*, **13**, 1461–1470.
27. Shi, W., Dirim, F., Wolf, E., Zakhartchenko, V. and Haaf, T. (2004) Methylation reprogramming and chromosomal aneuploidy in in vivo

fertilized and cloned rabbit preimplantation embryos. *Biol. Reprod.*, **71**, 340–347.
28. Fulka, H., Mrazek, M., Tepla, O. and Fulka, J. Jr (2004) DNA methylation pattern in human zygotes and developing embryos. *Reproduction*, **128**, 703–708.
29. Aranyi, T. and Paldi, A. (2006) The constant variation: DNA methylation changes during preimplantation development. *FEBS Lett.*, **580**, 6521–6526.
30. Beaujean, N., Hartshorne, G., Cavilla, J., Taylor, J., Gardner, J., Wilmut, I., Meehan, R. and Young, L. (2004) Non-conservation of mammalian preimplantation methylation dynamics. *Curr. Biol*, **14**, R266–R267.
31. Jedrusik, A., Parfitt, D.E., Guo, G., Skamagki, M., Grabarek, J.B., Johnson, M.H., Robson, P. and Zernicka-Goetz, M. (2008) Role of Cdx2 and cell polarity in cell allocation and specification of trophectoderm and inner cell mass in the mouse embryo. *Genes Dev.*, **22**, 2692–2706.
32. Tang, F., Barbacioru, C., Wang, Y., Nordman, E., Lee, C., Xu, N., Wang, X., Bodeau, J., Tuch, B.B., Siddiqui, A. *et al.* (2009) mRNA-Seq whole-transcriptome analysis of a single cell. *Nat. Methods*, **6**, 377–382.
33. Wang, H., Huang, Z.Q., Xia, L., Feng, Q., Erdjument-Bromage, H., Strahl, B.D., Briggs, S.D., Allis, C.D., Wong, J., Tempst, P. *et al.* (2001) Methylation of histone H4 at arginine 3 facilitating transcriptional activation by nuclear hormone receptor. *Science*, **293**, 853–857.
34. Pal, S., Vishwanath, S.N., Erdjument-Bromage, H., Tempst, P. and Sif, S. (2004) Human SWI/SNF-associated PRMT5 methylates histone H3 arginine 8 and negatively regulates expression of ST7 and NM23 tumor suppressor genes. *Mol. Cell Biol.*, **24**, 9630–9645.
35. Goto, H., Yasui, Y., Nigg, E.A. and Inagaki, M. (2002) Aurora-B phosphorylates Histone H3 at serine28 with regard to the mitotic chromosome condensation. *Genes Cells*, **7**, 11–17.
36. Qian, W., Choi, S., Gibson, G.A., Watkins, S.C., Bakkenist, C.J. and Van Houten, B. (2012) Mitochondrial hyperfusion induced by loss of the fission protein Drp1 causes ATM-dependent G2/M arrest and aneuploidy through DNA replication stress. *J. Cell Sci.*, **125**, 5745–5757.
37. Crosio, C., Fimia, G.M., Loury, R., Kimura, M., Okano, Y., Zhou, H., Sen, S., Allis, C.D. and Sassone-Corsi, P. (2002) Mitotic phosphorylation of histone H3: spatio-temporal regulation by mammalian Aurora kinases. *Mol. Cell Biol.*, **22**, 874–885.
38. Cascone, A., Bruelle, C., Lindholm, D., Bernardi, P. and Eriksson, O. (2012) Destabilization of the outer and inner mitochondrial membranes by core and linker histones. *PLoS One*, **7**, e35357.
39. Kim, J.M., Liu, H., Tazaki, M., Nagata, M. and Aoki, F. (2003) Changes in histone acetylation during mouse oocyte meiosis. *J. Cell Biol.*, **162**, 37–46.
40. Ribeiro-Mason, K., Boulesteix, C., Fleurot, R., Aguirre-Lavin, T., Adenot, P., Gall, L., Debey, P. and Beaujean, N. (2012) H3S10 phosphorylation marks constitutive heterochromatin during interphase in early mouse embryos until the 4-cell stage. *J. Reprod. Dev.*, **58**, 467–475.
41. Srinivasan, M., Sedmak, D. and Jewell, S. (2002) Effect of fixatives and tissue processing on the content and integrity of nucleic acids. *Am. J. Pathol.*, **161**, 1961–1971.
42. Schnell, U., Dijk, F., Sjollema, K.A. and Giepmans, B.N. (2012) Immunolabeling artifacts and the need for live-cell imaging. *Nat. Methods*, **9**, 152–158.
43. Summerton, J.E. (2007) Morpholino, siRNA, and S-DNA compared: impact of structure and mechanism of action on off-target effects and sequence specificity. *Curr. Top. Med. Chem.*, **7**, 651–660.
44. Bettencourt-Dias, M., Giet, R., Sinka, R., Mazumdar, A., Lock, W.G., Balloux, F., Zafiropoulos, P.J., Yamaguchi, S., Winter, S., Carthew, R.W. *et al.* (2004) Genome-wide survey of protein kinases required for cell cycle progression. *Nature*, **432**, 980–987.
45. Leonhardt, H., Page, A.W., Weier, H.U. and Bestor, T.H. (1992) A targeting sequence directs DNA methyltransferase to sites of DNA replication in mammalian nuclei. *Cell*, **71**, 865–873.
46. Yang, F., Camp, D.G. 2nd, Gritsenko, M.A., Luo, Q., Kelly, R.T., Clauss, T.R., Brinkley, W.R., Smith, R.D. and Stenoien, D.L. (2007) Identification of a novel mitotic phosphorylation motif associated with protein localization to the mitotic apparatus. *J. Cell Sci.*, **120**, 4060–4070.
47. Vakifahmetoglu, H., Olsson, M. and Zhivotovsky, B. (2008) Death through a tragedy: mitotic catastrophe. *Cell Death Differ.*, **15**, 1153–1162.
48. Vanneste, E., Voet, T., Le Caignec, C., Ampe, M., Konings, P., Melotte, C., Debrock, S., Amyere, M., Vikkula, M., Schuit, F. *et al.* (2009) Chromosome instability is common in human cleavage-stage embryos. *Nat. Med.*, **15**, 577–583.
49. Johnson, D.S., Gemelos, G., Baner, J., Ryan, A., Cinnioglu, C., Banjevic, M., Ross, R., Alper, M., Barrett, B., Frederick, J. *et al.* (2010) Preclinical validation of a microarray method for full molecular karyotyping of blastomeres in a 24-h protocol. *Hum. Reprod.*, **25**, 1066–1075.
50. Wiggin, G.R., Soloaga, A., Foster, J.M., Murray-Tait, V., Cohen, P. and Arthur, J.S. (2002) MSK1 and MSK2 are required for the mitogen- and stress-induced phosphorylation of CREB and ATF1 in fibroblasts. *Mol. Cell Biol.*, **22**, 2871–2881.
51. Soloaga, A., Thomson, S., Wiggin, G.R., Rampersaud, N., Dyson, M.H., Hazzalin, C.A., Mahadevan, L.C. and Arthur, J.S. (2003) MSK2 and MSK1 mediate the mitogen- and stress-induced phosphorylation of histone H3 and HMG-14. *EMBO J.*, **22**, 2788–2797.
52. Ikura, T., Ogryzko, V.V., Grigoriev, M., Groisman, R., Wang, J., Horikoshi, M., Scully, R., Qin, J. and Nakatani, Y. (2000) Involvement of the TIP60 histone acetylase complex in DNA repair and apoptosis. *Cell*, **102**, 463–473.
53. Gehani, S.S., Agrawal-Singh, S., Dietrich, N., Christophersen, N.S., Helin, K. and Hansen, K. (2010) Polycomb group protein displacement and gene activation through MSK-dependent H3K27me3S28 phosphorylation. *Mol. Cell*, **39**, 886–900.
54. Anderson, R.A., Bayne, R.A., Gardner, J. and De Sousa, P.A. (2010) Brain-derived neurotrophic factor is a regulator of human oocyte maturation and early embryo development. *Fertil. Steril.*, **93**, 1394–1406.
55. Ye, Y., Kawamura, K., Sasaki, M., Kawamura, N., Groenen, P., Sollewijn Gelpke, M.D., Kumagai, J., Fukuda, J. and Tanaka, T. (2009) Leptin and ObRa/MEK signalling in mouse oocyte maturation and preimplantation embryo development. *Reprod. Biomed. Online*, **19**, 181–190.
56. McElroy, S.L., Byrne, J.A., Chavez, S.L., Behr, B., Hsueh, A.J., Westphal, L.M. and Reijo Pera, R.A. (2010) Parthenogenic blastocysts derived from cumulus-free in vitro matured human oocytes. *PLoS One*, **5**, e10979.
57. Bruhat, A., Cherasse, Y., Maurin, A.C., Breitwieser, W., Parry, L., Deval, C., Jones, N., Jousse, C. and Fafournoux, P. (2007) ATF2 is required for amino acid-regulated transcription by orchestrating specific histone acetylation. *Nucleic Acids Res.*, **35**, 1312–1321.
58. Rho, J., Choi, S., Seong, Y.R., Cho, W.K., Kim, S.H. and Im, D.S. (2001) Prmt5, which forms distinct homo-oligomers, is a member of the protein-arginine methyltransferase family. *J. Biol. Chem.*, **276**, 11393–11401.
59. Kimura, A. and Horikoshi, M. (1998) Tip60 acetylates six lysines of a specific class in core histones in vitro. *Genes Cells*, **3**, 789–800.
60. Schultz, D.C., Ayyanathan, K., Negorev, D., Maul, G.G. and Rauscher, F.J. 3rd (2002) SETDB1: a novel KAP-1-associated histone H3, lysine 9-specific methyltransferase that contributes to HP1-mediated silencing of euchromatic genes by KRAB zinc-finger proteins. *Genes Dev.*, **16**, 919–932.
61. Doherty, A.S., Bartolomei, M.S. and Schultz, R.M. (2002) Regulation of stage-specific nuclear translocation of Dnmt1o during preimplantation mouse development. *Dev. Biol.*, **242**, 255–266.
62. Chen, T., Ueda, Y., Xie, S. and Li, E. (2002) A novel Dnmt3a isoform produced from an alternative promoter localizes to euchromatin and its expression correlates with active de novo methylation. *J. Biol. Chem.*, **277**, 38746–38754.
63. Cirio, M.C., Martel, J., Mann, M., Toppings, M., Bartolomei, M., Trasler, J. and Chaillet, J.R. (2008) DNA methyltransferase 1o functions during preimplantation development to preclude a profound level of epigenetic variation. *Dev. Biol.*, **324**, 139–150.
64. Hammoud, S.S., Nix, D.A., Zhang, H., Purwar, J., Carrell, D.T. and Cairns, B.R. (2009) Distinctive chromatin in human sperm packages genes for embryo development. *Nature*, **460**, 473–478.
65. Sendler, E., Johnson, G.D., Mao, S.H., Goodrich, R.J., Diamond, M.P., Hauser, R. and Krawetz, S.A. (2013) Stability, delivery and functions of human sperm RNAs at fertilization. *Nucleic Acids Res.*, **41**, 4104–4117.
66. Ananieva, O., Darragh, J., Johansen, C., Carr, J.M., McIlrath, J., Park, J.M., Wingate, A., Monk, C.E., Toth, R., Santos, S.G. *et al.* (2008) The kinases MSK1 and MSK2 act as negative regulators of Toll-like receptor signaling. *Nat. Immunol.*, **9**, 1028–1036.
67. Cui, X., Ji, D., Fisher, D.A., Wu, Y., Briner, D.M. and Weinstein, E.J. (2011) Targeted integration in rat and mouse embryos with zinc-finger nucleases. *Nat. Biotechnol.*, **29**, 64–67.
68. Wefers, B., Panda, S.K., Ortiz, O., Brandl, C., Hensler, S., Hansen, J., Wurst, W. and Kuhn, R. (2013) Generation of targeted mouse mutants by embryo microinjection of TALEN mRNA. *Nat. Protoc.*, **8**, 2355–2379.
69. Casanova, E., Fehsenfeld, S., Greiner, E., Stewart, A.F. and Schutz, G. (2002) Construction of a conditional allele of RSK-B/MSK2 in the mouse. *Genesis*, **32**, 158–160.
70. Giet, R. and Glover, D.M. (2001) Drosophila aurora B kinase is required for histone H3 phosphorylation and condensin recruitment during chromosome condensation and to organize the central spindle during cytokinesis. *J. Cell Biol.*, **152**, 669–682.

71. Lightfoot, D.A., Kouznetsova, A., Mahdy, E., Wilbertz, J. and Hoog, C. (2006) The fate of mosaic aneuploid embryos during mouse development. *Dev. Biol.*, **289**, 384–394.
72. Wei, Y., Mizzen, C.A., Cook, R.G., Gorovsky, M.A. and Allis, C.D. (1998) Phosphorylation of histone H3 at serine 10 is correlated with chromosome condensation during mitosis and meiosis in Tetrahymena. *Proc. Natl Acad. Sci. USA*, **95**, 7480–7484.
73. Vigneron, S., Brioudes, E., Burgess, A., Labbe, J.C., Lorca, T. and Castro, A. (2010) RSK2 is a kinetochore-associated protein that participates in the spindle assembly checkpoint. *Oncogene*, **29**, 3566–3574.
74. Kalista, T., Freeman, H.A., Behr, B., Reijo Pera, R.A. and Scott, C.T. (2011) Donation of embryos for human development and stem cell research. *Cell Stem Cell*, **8**, 360–362.
75. Hellemans, J., Mortier, G., De Paepe, A., Speleman, F. and Vandesompele, J. (2007) qBase relative quantification framework and software for management and automated analysis of real-time quantitative PCR data. *Genome Biol.*, **8**, R19.
76. Foygel, K., Choi, B., Jun, S., Leong, D.E., Lee, A., Wong, C.C., Zuo, E., Eckart, M., Reijo Pera, R.A., Wong, W.H. *et al.* (2008) A novel and critical role for Oct4 as a regulator of the maternal-embryonic transition. *PLoS One*, **3**, e4109.